Earth and Planetary Science Letters 269 (2008) 575-583

Contents lists available at ScienceDirect

Earth and Planetary Science Letters

journal homepage: www.elsevier.com/locate/epsl

Coccolithophore cell size and the Paleogene decline in atmospheric CO_2

Jorijntje Henderiks [a,*], Mark Pagani [b]

[a] Department of Geology and Geochemistry, Stockholm University, SE-106 91, Stockholm, Sweden
[b] Department of Geology and Geophysics, Yale University, P.O. Box 208109, New Haven, CT 06520, USA

ARTICLE INFO

Article history:
Received 30 November 2007
Received in revised form 26 February 2008
Accepted 4 March 2008
Available online 18 March 2008

Editor: R.D. van der Hilst

Keywords:
Coccolithophores
Coccolith biometry
Alkenones
Atmospheric CO2
Cenozoic
Evolution

ABSTRACT

Alkenone-based Cenozoic records of the partial pressure of atmospheric carbon dioxide (pCO_2) are founded on the carbon isotope fractionation that occurred during marine photosynthesis ($\varepsilon_{p37:2}$). However, the magnitude of $\varepsilon_{p37:2}$ is also influenced by phytoplankton cell size — a consideration lacking in previous alkenone-based CO_2 estimates. In this study, we reconstruct cell size trends in ancient alkenone-producing coccolithophores (the reticulofenestrids) to test the influence that cell size variability played in determining $\varepsilon_{p37:2}$ trends and pCO_2 estimates during the middle Eocene to early Miocene. At the investigated deep-sea sites, the reticulofenestrids experienced high diversity and largest mean cell sizes during the late Eocene, followed by a long-term decrease in maximum cell size since the earliest Oligocene. Decreasing haptophyte cell sizes do not account for the long-term increase in the stable carbon isotopic composition of alkenones and associated decrease in $\varepsilon_{p37:2}$ values during the Paleogene, supporting the conclusion that the secular pattern of $\varepsilon_{p37:2}$ values is primarily controlled by decreasing CO_2 concentration since the earliest Oligocene. Further, given the physiology of modern alkenone producers, and considering the timings of coccolithophorid cell size change, extinctions, and changes in reconstructed pCO_2 and temperature, we speculate that the selection of smaller reticulofenestrid cells during the Oligocene primarily reflects an adaptive response to increased $[CO_{2(aq)}]$ limitation.

1. Introduction

Carbon dioxide is one of the primary agents influencing climate over Earth history (Berner and Kothavala, 2001), with low levels of pCO_2 associated with lower global temperatures and increased ice volume. Well-constrained reconstructions of past levels of atmospheric CO_2 are therefore critical in evaluating the factors driving past climatic and paleoceanographic change. The alkenone-based pCO_2 method reconstructs the concentration of aqueous CO_2 ($CO_{2(aq)}$) in ocean surface waters using the stable carbon isotopic composition of C_{37} di-unsaturated alkenones ($\delta^{13}C_{alk}$) and estimates of the carbon isotopic fractionation ($\varepsilon_{p37:2}$) that occurred during marine algal photosynthesis (Bidigare et al., 1997,1999; Pagani et al., 2005), under the assumption that alkenone-producing haptophytes assimilate CO_2 predominantly by passive diffusion. Indeed, even though the modern coccolithophore *Emiliania huxleyi* evolved in a low-pCO_2 Pleistocene world, modern strains do not possess an efficient carbon concentrating mechanism (CCM) (Rost et al., 2003), causing haptophytes to be more sensitive to low $[CO_{2(aq)}]$ than other marine algae with efficient CCMs (Raven and Johnston, 1991; Badger et al., 1998). The magnitude of $\varepsilon_{p37:2}$ in the sedimentary record is a function of various factors including $[CO_{2(aq)}]$, algal growth rates (μ) (Bidigare et al., 1997) and the ratio of cellular carbon content to cell surface area (Popp et al., 1998) during late-stage exponential and stationary growth (Benthien et al., 2007).

Interpretations of ancient $\varepsilon_{p37:2}$ values generally assume that alkenone-producing algal cell volume to surface area (cell size) remained relatively constant over time (Pagani et al., 2005). However, a recent biometric analysis of coccoliths – calcitic scales that surround coccolithophore cells – determined that substantial changes in haptophyte cell size occurred during the early Miocene that likely influenced the magnitude of $\varepsilon_{p37:2}$ (Henderiks and Pagani, 2007).

In this study, we determine statistically robust trends in the dimensions of fossil coccolith assemblages and evaluate long-term trends in the cellular dimensions of ancient alkenone-producing algae (the reticulofenestrids) during the Paleogene. These data are then used to re-evaluate the magnitude of previously published middle Eocene to early Miocene $\varepsilon_{p37:2}$ values and pCO_2 estimates derived from the same ocean localities. In addition, we discuss the potential environmental factors driving the observed changes in cell size of reticulofenestrid assemblages at the investigated deep-sea sites.

2. Study sites and samples

For this study, 52 samples were selected from pelagic oozes and chalks recovered at two deep-sea drill sites, with sampling depths

* Corresponding author. Tel.: +46 8 674 78 32; fax: +46 8 674 78 97.
E-mail address: jorijntje.henderiks@geo.su.se (J. Henderiks).

0012-821X/$ – see front matter © 2008 Elsevier B.V. All rights reserved.
doi:10.1016/j.epsl.2008.03.016

corresponding to published alkenone-based $\varepsilon_{p37:2}$ data (Pagani et al., 2005; Fig. 1). Deep Sea Drilling Program (DSDP) Site 516 (western South Atlantic, Rio Grande Rise, 30°16.59′S, 35°17.10′W, currently at 1313 m water depth) provides well-preserved nannofossil assemblages covering the latest Eocene to early Miocene period (~34.6–16.8 Ma). Samples from DSDP Site 612 (western North Atlantic, continental slope off New Jersey, 38°49.21′N, 72°46.43′W, present water depth of 1404 m) cover the middle-late Eocene period (~44.5–34.1 Ma). For the latter site, we adopted a revised age model from that used in Pagani et al. (2005) to account for a hiatus at 181.39 mbsf, which corresponds to a tektite layer (e.g. Miller et al., 1991; see Table S1 in the Appendix). All paleoceanographic records discussed in this study are on a common geomagnetic polarity time scale (GPTS) (Cande and Kent, 1995; Berggren et al., 1995).

3. Methodology

3.1. Coccolith biometry

In today's open ocean, alkenone production appears restricted to the coccolith-bearing haptophyte species *E. huxleyi* and *Gephyrocapsa oceanica* (Marlowe et al., 1990; Conte et al., 1995). Another modern alkenone-producing but noncalcifying haptophyte, *Isochrysis galbana*, is restricted to coastal areas and therefore not likely to represent an important source of alkenones in deep-sea sediments (Marlowe et al., 1990). Modern descendants of common fossil Cenozoic lineages, such as *Coccolithus pelagicus* and *Calcidiscus leptoporus*, are not known to produce alkenones (Marlowe et al., 1990; Volkman, 2000). Importantly, all known alkenone-producing haptophytes group within the order Isochrysidales and are phylogenetically far removed from all other extant coccolithophores (Fujiwara et al., 2001; Sáez et al., 2004; Medlin et al., 2007). The ability to produce alkenones most likely evolved only once in (bloom-forming?) haptophytes, and recent molecular clock studies (Medlin et al., 2007) place the divergence between the Isochrysidales and other coccolithophores at ~195 Ma, before the first sedimentary evidence of alkenones in Cretaceous black shales at ~120 Ma (Farrimond et al., 1986; Brassell et al., 2004). *E. huxleyi* and *G. oceanica* have Pleistocene origins, and their Cenozoic ancestors are identified within the *Reticulofenestra* genus (family Noelaerhabdaceae) based on their co-occurrence with sedimentary alkenones and characteristic coccolith crystallography (Marlowe et al., 1990; Young et al., 1992). Hence, we focus our analysis on all combined morphospecies within the *Reticulofenestra* genus, providing an integrated signal of species diversity and total size range of the most probable ancient alkenone-producing algae.

Nannofossil census counts (>550 counts per sample) provide a measure of (morpho)species diversity expressed by the Shannon index (e.g. Pielou, 1969), which is a normalized measure that accounts for both species richness (the number of species in an assemblage) and the evenness of the species (i.e. the relative degree of species dominance). The most dominant coccolithophore genera include *Reticulofenestra*, *Cyclicargolithus* and *Coccolithus*. *Reticulofenestra* spp. dominate most assemblages with an average abundance of ~50% and peak abundances reaching ~80%. Only few Oligocene samples contain assemblages dominated by *Cyclicargolithus* (>50%; 5 out of 16 samples between 24–29 Ma). *Coccolithus* spp. are consistently present throughout the investigated interval, with and average abundance of ~14% and maximum abundance of 35%.

In each sample, reticulofenestrid size variability was determined by measuring ~200 individual coccoliths on four replicate slides (Henderiks and Törner, 2006). Each individual coccolith was identified at morphospecies level. Dimensional characteristics of intact fossil coccospheres and adjoining coccoliths reveal a robust linear relationship between coccolith length ($L_{coccolith}$) and coccolithophore cell diameter (D_{cell}) (r^2=0.82, p-value <0.0001; Henderiks and Pagani, 2007), allowing ancient coccolithophore cell sizes to be estimated from individual coccolith size measurements by the relationship:

$$D_{cell} = 0.55 + 0.88\, L_{coccolith}. \quad (1)$$

3.2. Cell size corrections to paleo-co_2 estimates

Larger phytoplankton cells, with higher carbon cell quota (which is proportional to cell volume) relative to surface area, discriminate less

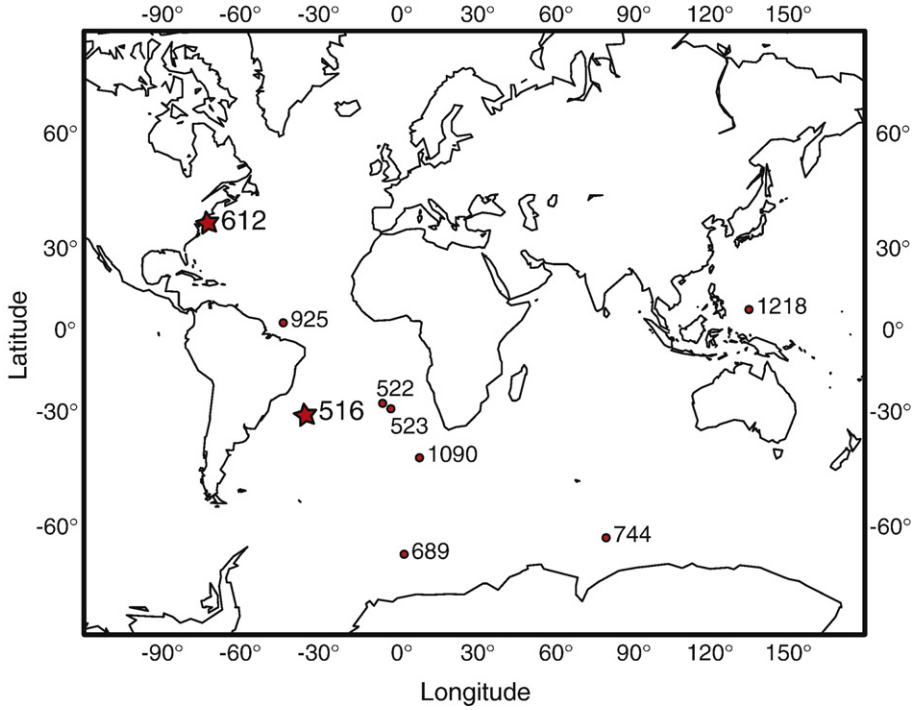

Fig. 1. Geographic locations of deep-sea sites used in this study. Records of long-term variability in reticulofenestrid cell size and alkenone isotopic values are derived from Deep Sea Drilling Program (DSDP) sites 516 and 612 (stars). Proxy records from additional DSDP and Ocean Drilling Program (ODP) sites (dots) are discussed in the text.

against ^{13}C than smaller cells under similar $CO_{2(aq)}$ (e.g. Laws et al., 1995; Popp et al., 1998). Accordingly, mean reticulofenestrid cell diameter estimates were converted to volume-to-surface area ratios (V:SA) assuming spherical geometry, and then used to reinterpret the alkenone-based $\varepsilon_{p37:2}$ values and estimates of $CO_{2(aq)}$ (Henderiks and Pagani, 2007). Summarizing, the magnitude of $\varepsilon_{p37:2}$ is directly proportional to the ratio of cellular volume to surface area:

$$\varepsilon_p = \varepsilon_f - \frac{b}{CO_{2(aq)}} \quad (2)$$

where the term '*b*' represents the sum of all physiological factors affecting carbon discrimination, such as growth rate (μ) and cell geometry (V:SA). The magnitude of the term *b* is estimated by the phosphate concentration of the surface ocean at any particular site (Bidigare et al., 1997, 1999; Pagani et al., 2005). In localities with low, relatively invariable [PO_4^{3-}], such as sites 516 and 612 (0.2–0.4 and 0.3–0.5 μM, respectively), the influence of haptophyte growth rates on the magnitude of $\varepsilon_{p37:2}$ is assumed negligible. Thus, for this study, the term *b* is adjusted relative to changes in V:SA of ancient haptophytes, such that:

$$b' = b\left[\frac{V:SA_{fossil}}{V:SA_{Ehux}}\right] \quad (3)$$

where $V:SA_{fossil}$ is estimated from mean coccolith size in each sample, and $V:SA_{Ehux}$ is a constant value reflecting cell dimensions of the modern haptophyte *E. huxleyi* in chemostat culture, with mean cell $V:SA_{Ehux} = 0.9 \pm 0.1$ μm (Popp et al., 1998). Values for ancient $CO_{2(aq)}$ are calculated from $\varepsilon_{p37:2}$, $\varepsilon_f = 25‰$ and the revised term *b*' (Eqs. (2) and (3)), and converted to pCO_2 by applying Henry's Law assuming a salinity of 35 and surface water temperatures derived from $\delta^{18}O$ of marine carbonates. This approach is similar to that used by Pagani et al. (1999, 2005) in estimating past $CO_{2(aq)}$ and pCO_2, but now includes a factor for variable cell geometry.

4. Results

Maximum reticulofenestrid coccolith size and the total coccolith size range (as depicted by the 5th–95th percentile sizes) are largest during the late Eocene and earliest Oligocene when $\delta^{13}C_{alk}$ values are most negative, at both investigated sites (Fig. 2). Independent size data for the largest morphospecies *Reticulofenestra umbilica* (DSDP site 523; Backman and Hermelin, 1986) support the 95th percentile size values observed in this study (Fig. 2B), indicating that our regional records of 'lumped' size measurements faithfully represent the maximum size range in reticulofenestrids during the Eocene and earliest Oligocene. At site 516, maximum reticulofenestrid size and total coccolith range progressively decrease during the Oligocene and early Miocene, associated with an increase in $\delta^{13}C_{alk}$ values (Figs. 2A–B). Distinct decreases in reticulofenestrid diversity largely reflect assemblages dominated by small morphospecies (Events 1–4; Fig. 2B–C). The consistent presence and preservation of small coccoliths implies that preferential dissolution and/or winnowing (of thin, small liths) had minor influence on our reticulofenestrid size records. Diagenetic calcite overgrowth of coccoliths was not observed. Mean coccolith size is strongly correlated to maximum observed length ($r = 0.79$; p-value < 0.0001), while its correlation to minimum size is not statistically significant ($r = 0.16$; p-value $= 0.247$). This indicates that the abundance of large morphospecies substantially influence the observed size patterns, with no evidence for a directional change in minimum size. Indeed, the relative contributions of the largest reticulofenestrid morphospecies, *R. umbilica* and *R. bisecta* (Fig. 2D), strongly covary with mean reticulofenestrid size and diversity during the Paleogene.

Both $\varepsilon_{p37:2}$ and calculated mean V:SA values show a long-term decrease since the early Oligocene (Fig. 3). Importantly, this long-term size decrease is punctuated by rapid step-like changes including substantial decreases in mean reticulofenestrid size, depicting periods when small reticulofenestrids are dominant (Events 1–4). For example, Event 1 is depicted by a ~40% decrease in mean reticulofenestrid size (~7.9 μm to 4.7 μm) at site 516 between ~34–33 Ma, which is closely associated with a rapid shift in deep-sea $\delta^{18}O$ at the E–O transition (Zachos et al., 1996; Coxall et al., 2005), but lacks substantial changes in $\delta^{13}C_{alk}$ (Fig. 2A) or related $\varepsilon_{p37:2}$ (Fig. 3A). Event 2, between 28–29 Ma, also indicates a period of dominance by small reticulofenestrids, although the alkenone record is less well resolved during this time. By contrast, distinctly elevated $\varepsilon_{p37:2}$ values correspond to dominance by small reticulofenestrids at ~25 Ma and ~21–20 Ma (Events 3–4). This correspondence suggests that small cell sizes have, in part, helped to magnify the 2–4‰ increases in $\varepsilon_{p37:2}$, during these times (Fig. 3A), whereas large cell sizes would have attenuated the magnitude of $\varepsilon_{p37:2}$ values during the latest Eocene.

5. Discussion

5.1. Evaluation of alkenone records

The $\varepsilon_{p37:2}$ values of the late Eocene–earliest Oligocene are greater than any observed in the modern ocean (Pagani et al., 2005). Within the bounds of the published approach to interpreting $\varepsilon_{p37:2}$ (Bidigare et al., 1997; Pagani et al., 2005), this would imply either that (1) reticulofenestrid cell sizes were much smaller than modern *E. huxleyi*, (2) haptophyte growth rates were substantially lower than the lowest rates observed in oligotrophic parts of the modern ocean, or (3) CO_2 levels were higher. Our results indicate that the major features of the published CO_2 record, including the high $\varepsilon_{p37:2}$ values of the middle Eocene–early Oligocene and the secular trends in $\delta^{13}C_{alk}$ and $\varepsilon_{p37:2}$, cannot be interpreted as a cell size effect. Indeed, if cell size changes influenced alkenone isotope chemistry, it would have acted to minimize the magnitude of long-term isotopic change and, as a consequence, attenuate the magnitude of CO_2 change during the Eocene and Oligocene (Fig. 3B). On the other hand, short-term changes in $\delta^{13}C_{alk}$ and $\varepsilon_{p37:2}$ during the late Oligocene and early Miocene could be partly explained by changes in the mean cell size of alkenone-producing algae (cf. Henderiks and Pagani, 2007). For example, associated cell size decreases at ~25 Ma and ~21–20 Ma (Events 3–4), result in an overestimation of pCO_2 during these times: cell size revised paleo-CO_2 estimates are lower by ~100–300 ppmv with respect to values reported in Pagani et al. (2005) (Fig. 3D).

A scenario calling for a suppression of algal growth rates during the late Eocene–earliest Oligocene to explain elevated $\varepsilon_{p37:2}$ values does not appear reasonable. Eocene to earliest Oligocene $\varepsilon_{p37:2}$ values are substantially higher than those recorded from the modern oligotrophic waters where [PO_4^{3-}] ranges between 0.0 to 0.2 μmol/l. In terms of specific algal growth rates, this would imply that Paleogene alkenone producers had substantially lower growth rates than modern *E. huxleyi* in oligotrophic settings. However, the paleo-$\varepsilon_{p37:2}$ record is derived from both oligotrophic and eutrophic environments (Pagani et al., 2005). If algal growth rates were the primary reason for high Eocene $\varepsilon_{p37:2}$ values, then growth rates at eutrophic sites would have to be lower than those found in the gyre regions of the modern ocean.

The simplest explanation for the pattern of paleo-$\varepsilon_{p37:2}$ values calls on higher-than-modern CO_2 concentrations during the Eocene reaching near-modern CO_2 concentrations by the early Miocene (Pagani et al., 2005). If cell size variations are considered, larger mean reticulofenestrid V:SA during the late Eocene would imply even higher paleo-CO_2, increasing concentrations by ~100 to 400 ppmv above published values (Fig. 3D). Arguably, this effect could be amplified, if alkenones represent a comparable proportion of cell biomass among all reticulofenestrids — the contribution of alkenones by large cells would be proportionally larger than by small cells. However,

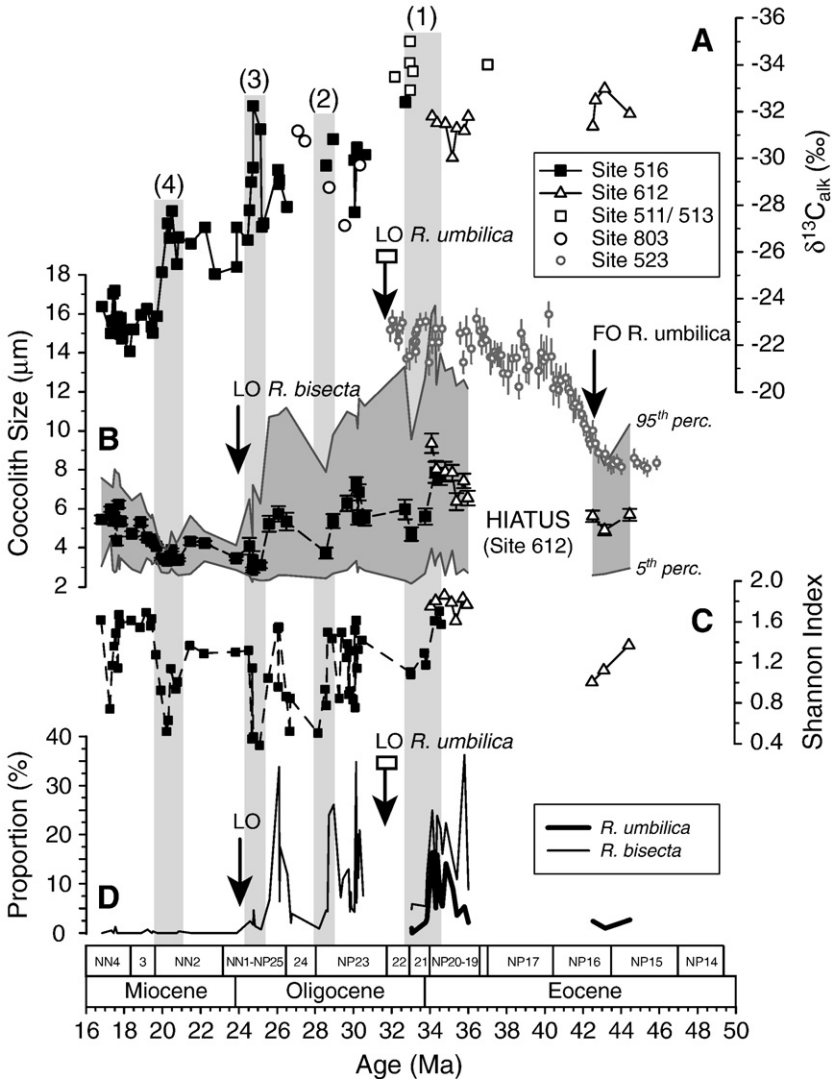

Fig. 2. Long-term variability in (A) alkenone $\delta^{13}C$ values (Pagani et al., 2005) and (B) coccolith size of ancient alkenone producers (μm) during the middle Eocene–early Miocene at Atlantic DSDP Sites 516 and 612. Note that data are plotted against a revised age model for Site 612, including a hiatus in the middle Eocene (Table S1 in the Appendix). Shown in (B) are mean (±95% confidence), as well as an envelope of 5th and 95th percentile sizes. Events (1)–(4) depict distinct minima in mean reticulofenstrid size. Arrows indicate the respective global first occurrence (FO) and last occurrence (LO) of *R. umbilica* (42.5 and 31.4–32.3 Ma, respectively) and *R. bisecta* (LO at 23.9 Ma). Mean coccolith size (±95% conf.) of *R. umbilica*, at DSDP Site 523 (28°S, 2°W), is adapted from Backman and Hermelin (1986). (C) Reticulofenestrid morphospecies diversity as expressed by the Shannon index. Low values depict assemblages of low species numbers and/or high degree of dominance by few species. (D) Relative abundance of the two largest morphospecies, *R. umbilica* and *R. bisecta*, within reticulofenestrid assemblages.

attempting to reconstruct and scale to ancient algal 'biomass' introduces large uncertainty, adding to an approach already built on many assumptions (Pagani et al., 2005; Sections 3.1–3.2). Nevertheless, the long-term character of atmospheric CO_2 estimates remains broadly similar to the previously published record regardless of the potential effect of changes in cell size.

According to model simulations, a gradual decline in pCO_2 during the late Eocene could have triggered Antarctic glaciation (DeConto and Pollard, 2003). However, cell size corrected, alkenone-based pCO_2 values appear to rise prior to the transition to "icehouse" conditions and fall rapidly after this climate event (Fig. 3D). Though intriguing, data resolution needs to be improved across this event to fully appreciate the relationship between CO_2 and polar ice growth during this time.

5.2. Targeting ancient alkenone producers

Alkenone-producing haptophyte species are members of the Isochrysidales clade, phylogenetically far removed from other coccolithophores (Medlin et al., 2007) — but not all Isochrysidales are known to produce alkenones (Marlowe et al., 1990). Therefore, it is possible that (1) all reticulofenestrids produced alkenones in the past, thus encompassing a range in cell sizes as discussed in the present study, or (2) only the smallest Cenozoic ancestors of similarly small-sized *Gephyrocapsa* and *Emiliania* produced alkenones. The latter scenario complies with the initial assumptions made by Pagani et al. (2005), that no or only minor cell size variability occurred during the Cenozoic that had no significant impact on the trends described by the $\varepsilon_{p37:2}$ record.

Arguably, we cannot preclude that the extinct genus *Cyclicargolithus* – with circular coccolith morphologies distinct from the elliptical reticulofenestrids (Henderiks, 2008) – could also have produced alkenones, since this genus is taxonomically grouped under the Isochrysidales (Young, 1998). This taxon is only a prominent contributor to the Oligocene nannofossil assemblages at site 516. We tested the influence of including *Cyclicargolithus* in our cell size considerations by combining our census counts and mean size data for *Reticulofenestra* and *Cyclicargolithus* across the Oligocene interval

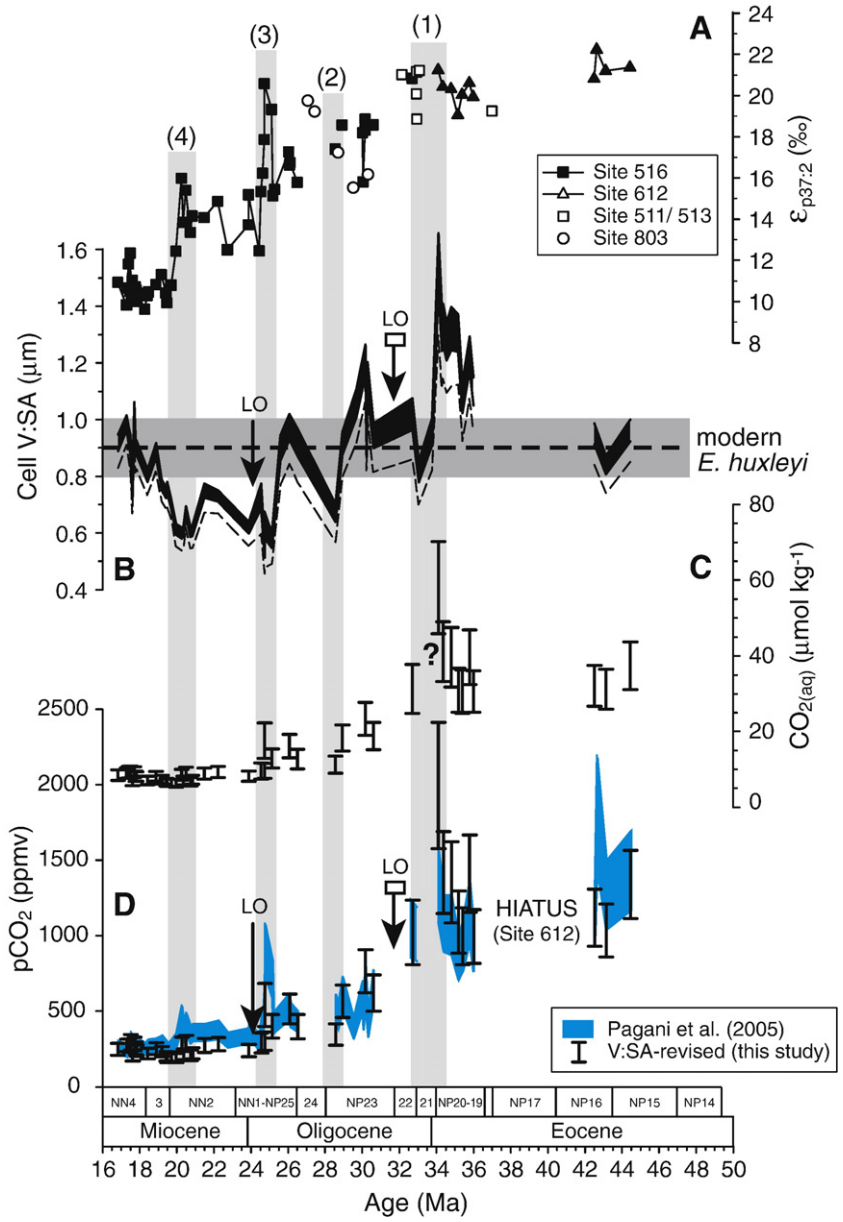

Fig. 3. Evaluation of the alkenone-derived paleo-$\varepsilon_{p37:2}$ record and V:SA-adjusted calculations of aqueous CO_2 concentrations ($CO_{2(aq)}$) and atmospheric levels of CO_2 (pCO_2) based on the temporal cell size variability of ancient alkenone-producing coccolithophores. Shown from left to right are (A) $\varepsilon_{p37:2}$ (‰; Pagani et al., 2005); (B) mean reticulofenestrid cell volume-to-surface area ratios (V:SA, in µm) calculated from mean coccolith length (±standard error) using Eq. (1). Black interval represents mean V:SA and propagated upper 95% confidence interval. Dashed line indicates propagated lower 95% confidence estimate. Grey horizontal band illustrates V:SA values of modern *E. huxleyi* (0.9±01 µm). Events (1)–(4), and species LO's as in Fig. 1. (C) V:SA-revised, $\varepsilon_{p37:2}$ derived estimates of [$CO_{2(aq)}$] (µmol kg^{-1}). In our re-evaluation of [$CO_{2(aq)}$], we propagated the 95% confidence intervals for V:SA, minimum and maximum estimates of $\varepsilon_{p37:2}$, and used constant ranges in [PO_4^{3-}] (Site 516: 0.2–0.4 µM; Site 612: 0.3–0.5 µM) to adjust estimates of the physiological term 'b' (Eqs. (2) and (3)); (D) V:SA-revised paleo-pCO_2 reconstructions (ppmv). Intervals represent minimum and maximum estimates with propagated 95% confidence levels of input factors. Conversion from [$CO_{2(aq)}$] into pCO_2 was achieved using Henry's Law and mean SST as determined by Pagani et al. (2005).

(24.5–32.7 Ma). This resulted in slightly higher mean cell size-adjusted estimates of CO_2 that fall largely within the given ranges using only reticulofenestrid data, and therefore does not impact our overall conclusions illustrated in Fig. 3D.

5.3. Cell size variability: ecology and evolution

Coccolithophorid cell size is likely influenced by a variety of passive and active selection pressures, with specific factors, such as resource availability and climatic change, determining trends over time. In addition, different forcings operate on ecologic to evolutionary time-scales. The correspondence between large (small) mean coccolith size and high (low) reticulofenestrid species diversity demonstrates that reticulofenestrid species composition – and thus regional coccolithophore ecology – is a major driving force of the observed size variability in our records on 100 to 400-ky time-scales (Fig. 2B–C; Events 1–4). To a lesser degree, intra-specific size variation of the main morphospecies in our samples influences the overall cell size compositions (Fig. 4). This potentially phenotypic size response suggests that additional biotic and/or abiotic factors affected the cell size, notably during the E–O transition when distinct decreases in cell size occurred in all morphospecies (Event 1).

On longer time-scales, a reduction in maximum size at sites 516 and 612 is also impacted by global extinctions of the largest reticulofenestrid morphospecies, and thus represents an evolutionary process (Figs. 4 and 5). In the South Atlantic (site 516) and Southern

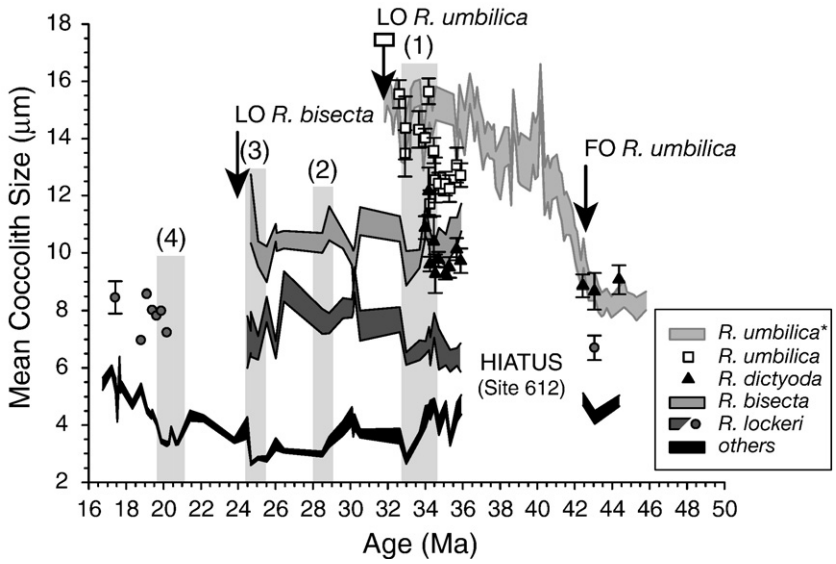

Fig. 4. Temporal variability in mean coccolith size (95% confidence intervals), for distinct morphospecies groups within the studied reticulofenestrid assemblages at Sites 516 and 612. FO, LO, and Events (1)–(4) as in Fig. 1. The evolutionary selection against large morphospecies may in part explain the overall decline in mean reticulofenestrid size during the Oligocene, while the evolution of the largest morphospecies *R. umbilica* (42.5 Ma; *adapted from Backman and Hermelin, 1986) from middle Eocene *R. dictyoda* appears to have influenced the observed mean size increase during the late Eocene. Still, each morphospecies group shows decreased mean size following Antarctic glaciation (at ~34 Ma), consistent with the marked mean reticulofenestrid size decrease across the E–O transition (Event 1).

Ocean (ODP sites 689 and 744; Persico and Villa, 2004), the relative abundance of *Reticulofenestra umbilica* strongly declined at ~34 Ma, coinciding with major climatic change of the E–O climate transition (Fig. 2D), but the global extinction of this cosmopolitan species occurred several million years later (mid-latitudes: 32.3 Ma; Berggren et al., 1995; Shackleton et al., 1999; high southern latitudes: 31.4 Ma; Persico and Villa, 2004). Similarly, the cosmopolitan *Reticulofenestra bisecta* suffered sharp decreases in abundance during the latest Eocene and Oligocene (Fig. 2D), the last of which (~25.5 Ma) occurred long before its global extinction during the latest Oligocene (23.9 Ma; Berggren et al., 1995). Both last occurrences (LO's) are conspicuously associated with distinct declines in $\varepsilon_{p37:2}$ values at ~32 Ma and ~24.5 Ma (Fig. 3A).

5.4. Abiotic forcing on plankton size?

In today's oligotrophic ocean regions, coccolithophore cell densities show strong seasonality and appear largely forced by abiotic, environmental parameters, such as nutrients, temperature and irradiance (Haidar and Thierstein, 2001; Cortés et al., 2001). A general allometric rule dictates that smaller unicellular phytoplankton cells have higher nutrient-uptake and growth rates because of their low V:SA ratios (Raven, 1998). Most modern oceanic coccolithophores appear to be adapted to low nutrient, non-variable environmental conditions, and do not respond to nutrient enrichment (Brand, 1994). By contrast, *E. huxleyi* and *G. oceanica* both have higher maximum growth rates and respond positively to nutrient enrichment (Hulburt, 1985; Brand, 1994; Haidar and Thierstein, 2001). For example, in the north Atlantic subtropical gyre system off Bermuda, *E. huxleyi* is the dominant coccolithophore from late winter to spring, when surface water stratification breaks down due to winter mixing and nutrients are supplied to the photic zone at low temperatures (Haidar and Thierstein, 2001). Similarly, it is probable that fast-growing, small reticulofenestrids that dominate Cenozoic nannofloral assemblages were better adapted, relative to larger taxa, in exploiting limited resources.

Finkel et al. (2005) postulated a scenario of decreasing whole-ocean nutrient availability resulting from long-term cooling and increased thermal stratification during the Cenozoic as the main cause of a macroevolutionary size decrease in diatoms, that appears most pronounced since the early Miocene. This conclusion was based on linear regression analysis of globally averaged diatom size (without regard to relative species abundances) and long-term, smoothed trends in the temperature contrast between the deep and surface ocean in the tropics (Wright, 2001) that were interpolated at 5-million year intervals (Finkel et al., 2005). However, a similar analysis of mean algal cell size and records of ocean stratification, from corresponding

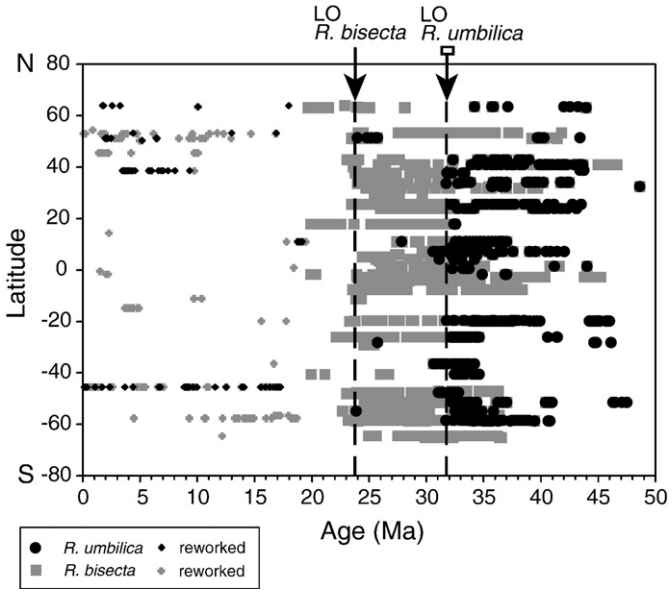

Fig. 5. Geographic distribution of *Reticulofenestra umbilica* (black symbols) and *R. bisecta* (grey symbols) over the last 50 Ma, illustrating cosmopolitan occurrence before their respective global extinctions (LO: last occurrence). Occurrences of each species were documented in DSDP and ODP samples at, respectively, 34 Sites (24 Legs) and 54 Sites (34 Legs) from the Atlantic, Indian and Pacific oceans, as compiled in the biostratigraphic NEPTUNE database (Spencer-Cervato, 1999). Rare occurrences in Neogene sediments are interpreted as reworking of fossil specimens, a process which appears most pronounced in high latitudes.

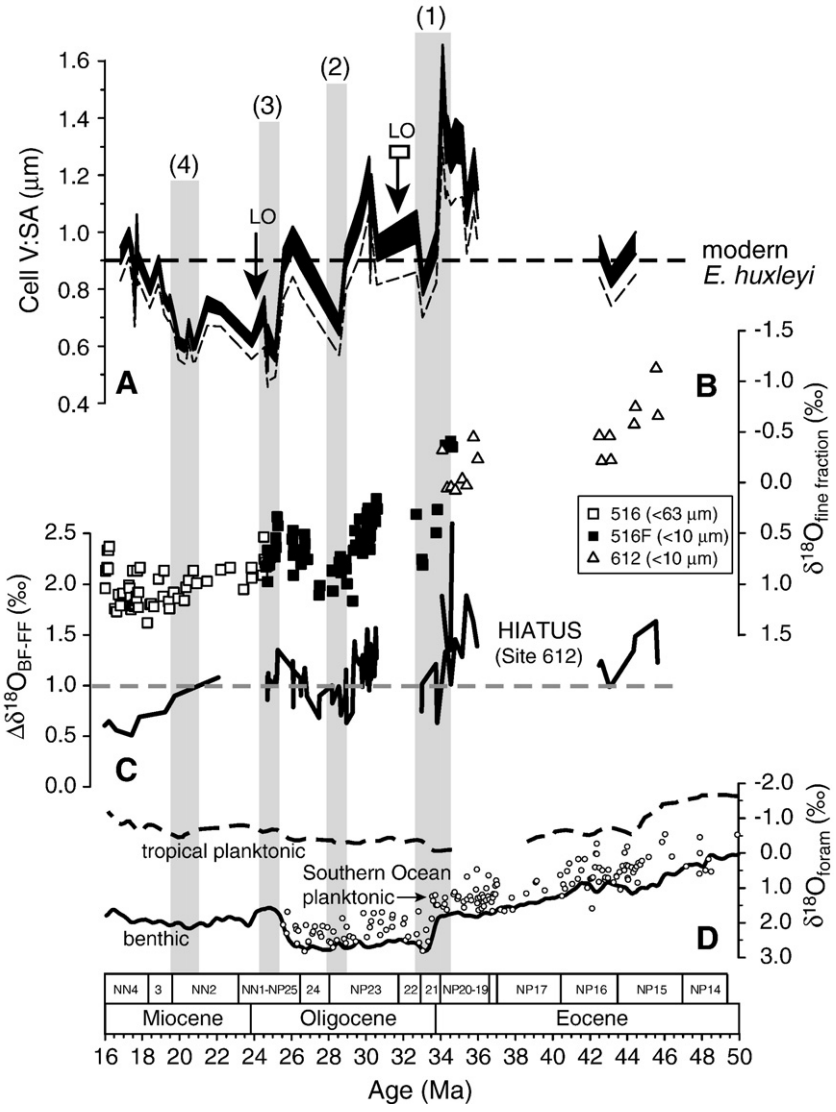

Fig. 6. (A) Mean reticulofenestrid cell volume-to-surface area ratios (V:SA, in µm; as Fig. 3B) compared to (B) coccolith-dominated fine fraction stable oxygen isotopic ratios ($\delta^{18}O_{FF}$ in ‰), representing late winter–early spring surface water conditions (Ennyu et al., 2002) and (C) gradients between benthic foraminiferal and fine fraction $\delta^{18}O$ ($\Delta\delta^{18}O_{BF-FF}$ in ‰) in corresponding samples at sites 612 and 516. The latter serves as a qualitative assessment of the thermal stratification of the ocean. Stable isotopic data at sites 612 and 516F adopted from Pagani et al. (2005), fine fraction isotopic data at site 516 (latest Oligocene–early Miocene) from Ennyu et al. (2002). (D) Long-term trends (lines: 1 m.y. Gaussian filter) of deep ocean and surface water stable oxygen isotopic composition in foraminifera; solid line: global benthic compilation (Zachos et al., 2001); dashed line: tropical planktonic values drawn after Wright (2001); open symbols: Southern Ocean planktonic (Mackensen and Ehrmann, 1992). Note that the long-term decrease in $\delta^{18}O_{FF}$ from the middle Eocene to early Miocene at sites 516 and 612 is consistent with global, long-term decreases in deep-ocean and high-latitude surface temperatures.

samples at Sites 516 and 612 (n=33), reveals contrasting results that do not support this hypothesis on a regional scale and/or higher temporal resolution (Fig. 6). Significant correlations between cell size estimates and the $\delta^{18}O$ of coccolith-dominated fine fraction ($\delta^{18}O_{FF}$) suggest a decrease in reticulofenestrid size with decreasing surface temperatures (r=0.63 and 0.69 for, respectively, mean V:SA and 95th percentile coccolith size; p-value≪0.0001). However, the regional isotopic gradients between benthic foraminiferal and fine fraction $\delta^{18}O$ ($\Delta\delta^{18}O_{BF-FF}$; Fig. 6C) suggest a reduction in ocean stratification from the late Eocene to early Miocene. Opposite to results presented in Finkel et al. (2005), our records indicate a decrease in mean V:SA with decreasing ocean stratification (estimated by $\Delta\delta^{18}O_{BF-FF}$; r=0.61, p-value<0.0002).

If nutrient availability was the main factor forcing plankton cell size over the Cenozoic, then the sharp shorter-term decrease in reticulofenestrid size across the E–O transition (Event 1) at oligotrophic site 516 should correspond to an increase in ocean stratification — opposite to what our data suggest (Fig. 6). In fact, evidence for regionally increased paleoproductivity, notably by diatoms, extends from the western equatorial Atlantic (ODP site 925: Nilsen et al., 2003) to the South Atlantic and Southern Ocean (e.g. ODP site 1090: Anderson and Delaney, 2005; ODP site 689: Diester-Haass and Zahn, 1996; Fig. 1) in association with climatic cooling during the E–O transition (e.g. Dupont-Nivet et al., 2007; Zanazzi et al., 2007), and is inconsistent with a reduction in nutrient availability. In addition, long-term cooling during the Eocene is paired with a directional increase (and not decrease) in cell size in *R. umbilica* (Backman and Hermelin, 1986; Fig. 2B), when our $\Delta\delta^{18}O_{BF-FF}$ record suggests periods of relatively strong thermal stratification (Fig. 6C). Therefore, we contend that the relationship between coccolithophore size and thermal stratification and/or nutrient availability, on evolutionary and shorter climatic time-scales, is not consistent with the model proposed by Finkel et al. (2005). Rather, the gradual decline in reticulofenestrid upper size and nannofloral extinctions in relation to changes in $\varepsilon_{p37:2}$ suggest that a fall in CO_2 was a primary factor forcing a long-term decrease in reticulofenestrid cell size during the Oligocene.

5.5. Co_2 forcing on coccolithophore size?

A stark contrast between an overall diversity increase in diatoms (Spencer-Cervato, 1999; Falkowski et al., 2004) and progressive loss of coccolithophorid diversity (Aubry, 1992; Bown, 2005) since the early Oligocene reflects fundamental differences in physiology and ecologic success of these two phytoplankton groups in the "icehouse" world. Diatoms possess highly efficient and regulated CCMs, in contrast to modern alkenone-producing *E. huxleyi* (Raven and Johnston, 1991; Badger et al., 1998; Rost et al., 2003). Notably, the catalytic efficiency of Rubisco appears evolutionary conservative within the major algal groups (Tortell, 2000). Indeed, the fact that a CCM is only weakly developed in modern *E. huxleyi* – an organism that originated and evolved under Pleistocene low levels of pCO_2 – supports the notion that its ancestors had similarly inefficient, or perhaps no need for CCMs under higher CO_2 levels during Paleogene times.

During the Eocene, when CO_2 was higher than today (Lowenstein and Demicco, 2006), we speculate that the characteristically large coccolithophore species, such as *R. umbilica* and *R. bisecta*, relied on a diffusive uptake of $CO_{2(aq)}$ for photosynthesis and growth — an energetically inexpensive physiological adaptation. Smaller reticulofenestrids, perhaps with a nascent CCM (Rost et al., 2003), subsequently had a competitive advantage over larger forms as CO_2 became increasingly limiting during the late Oligocene. Our data suggest that large, cosmopolitan reticulofenestrids became ecologically marginalized during rapid climatic change, such as during the E–O transition (Fig. 2D), but that cell growth and survival of the species was sustained until atmospheric pCO_2 crossed bio-limiting threshold values, associated with their respective global extinctions (Fig. 5). Intriguingly, the fact that *R. umbilica* first disappeared in the mid-latitudes (32.3 Ma) and later in the high latitudes (31.4 Ma) may relate to the fact that cooler polar waters are characterized by higher concentrations of dissolved CO_2.

6. Summary

Substantial changes in cell size of alkenone-producing coccolithophores, relative to modern *E. huxleyi*, occurred during the middle Eocene–early Miocene. However, cell size considerations do not alter the overall conclusions of alkenone-based paleo-pCO_2 reconstructions, but imply even higher pCO_2 concentrations just prior to the early Oligocene glaciation at ~34 Ma. A long-term size decrease in reticulofenestrids, with largest cell size and high species diversity during the "hothouse" Eocene and progressive loss of large morphospecies since the early "icehouse" Oligocene, is consistent with a secular decrease in pCO_2. A substantial decrease in pCO_2 during the early Oligocene would have enhanced carbon limitation, driving the selection of smaller coccolithophorid species characterized by a higher net influx of CO_2 relative to the organism's carbon cell quota.

On shorter time-scales, reticulofenestrid size appears influenced by climatic and ecologic variability, with distinct periods of time when small morphospecies dominated reticulofenestrid assemblages. For example, the abrupt Eocene–Oligocene climate shift and associated changes in ocean dynamics occurred at ~34 Ma and was characterized by a prompt contraction of reticulofenestrid cell sizes which recovered to larger size by ~33 Ma in the oligotrophic South Atlantic. Finally, we demonstrate that a recent hypothesis linking ocean thermal stratification and macroevolutionary size trends in marine phytoplankton (Finkel et al., 2005) cannot explain mean reticulofenestrid cell size variability on a regional and/or higher temporal resolution.

Acknowledgments

This study used Deep Sea Drilling Project samples provided by the Ocean Drilling Program. Research was supported by Swedish Research Council grant VR621-2003-3614 to J. Henderiks and NSF grant OCE-0095734 to M. Pagani. Published data were kindly provided by J. Backman and A. Ennyu. We thank our anonymous reviewers for their constructive comments that helped improve the manuscript.

Appendix A. Supplementary data

Supplementary data associated with this article can be found, in the online version, at doi:10.1016/j.epsl.2008.03.016.

References

Anderson, L.D., Delaney, M.L., 2005. Middle Eocene to early Oligocene paleoceanography from Agulhas Ridge, Southern Ocean (Ocean Drilling Program Leg 177, Site 1090). Paleoceanography 20 (PA1013). doi:10.1029/2004PA001043.

Aubry, M.-P., 1992. Late Paleogene calcareous nannoplankton evolution: a tale of climatic deterioration. In: Prothero, D.R., Berggren, W.A. (Eds.), Eocene–Oligocene Climatic and Biotic Evolution. Princeton University Press, Princeton, New Jersey, pp. 272–309.

Backman, J., Hermelin, J.O.R., 1986. Morphometry of the Eocene nannofossil *Reticulofenestra* umbilicus lineage and its biochronological consequences. Palaeogeography, Palaeoclimatology, Palaeoecology 57, 103–116.

Badger, M.R., Andrews, T.J., Whitney, S.M., Ludwig, M., Yellowlees, D.C., Leggat, W., Price, G.D., 1998. The diversity and coevolution of Rubisco, plastids, pyrenoids, and chloroplast-based CO_2-concentrating mechanisms in algae. Canadian Journal of Botany 76, 1052–1971.

Benthien, A., Zondervan, I., Engel, A., Hefter, J., Terbrüggen, A., Riebesell, U., 2007. Carbon isotopic fractionation during mesocosm bloom experiment dominated by *Emiliania huxleyi*: effects of CO_2 concentration and primary production. Geochimica et Cosmochimica Acta 71, 1528–1541.

Berggren, W.A., Kent, D.V., Swisher, C.C., Aubry, M.-P., 1995. A revised Cenozoic geochronology and chronostratigraphy. SEPM Special Publication 54, 129–212.

Berner, R.A., Kothavala, Z., 2001. GEOCARB III: a revised model of atmospheric CO_2 over Phanerozoic time. American Journal of Science 301, 182–204.

Bidigare, R.R., Fluegge, A., Freeman, K.H., Hanson, K.L., Hayes, J.M., Hollander, D., Jasper, J.P., King, L.L., Laws, E.A., Milder, J., Millero, F.J., Pancrost, R., Popp, B.N., Steinberg, P.A., Wakeham, S.G., 1997. Consistent fractionation of ^{13}C in nature and in the laboratory: growth-rate effects in some haptophyte algae. Global Biogeochemical Cycles 11 (2), 279–292.

Bidigare, R.R., et al., 1999. Correction to "consistent fractionation of ^{13}C in nature and in the laboratory: growth-rate effects in some haptophyte algae" by R.R. Bidigare et al. Global Biogeochemical Cycles 13 (1), 251–252.

Bown, P., 2005. Calcareous nannoplankton evolution: a tale of two oceans. Micropaleontology 51 (4), 299–308.

Brand, L., 1994. Physiological ecology of marine coccolithophores. In: Winter, A., Siesser, W.G. (Eds.), Coccolithophores. University Press, Cambridge, pp. 39–49.

Brassell, S.C., Dumitrescu, M., ODP Leg198 Shipboard Scientific Party, 2004. Recognition of alkenones in a lower Aptian porcellanite from the west-central Pacific. Organic Geochemistry 35, 181–188.

Cande, S.C., Kent, D.V., 1995. Revised calibration of the geomagnetic polarity timescale for the Late Cretaceous and Cenozoic. Journal of Geophysical Research 100 (B4), 6093–6095.

Conte, M., Thompson, A., Eglinton, G., Green, J.C., 1995. Lipid biomarker diversity in the coccolithophorid *Emiliania huxleyi* (Prymnesiophyceae) and the related species *Gephyrocapsa oceanica*. Journal of Phycology 31, 272–282.

Cortés, M.Y., Bollmann, J., Thierstein, H.R., 2001. Coccolithophore ecology at the HOT station ALOHA, Hawaii. Deep-Sea Research II 48, 1957–1981.

Coxall, H.K., Wilson, P.A., Pälike, H., Lear, C.H., Backman, J., 2005. Rapid stepwise onset of Antarctic glaciation and deeper calcite compensation in the Pacific Ocean. Nature 433, 53–57.

DeConto, R.M., Pollard, D., 2003. Rapid Cenozoic glaciation of Antarctica induced by declining atmospheric CO_2. Nature 421, 245–249.

Diester-Haass, L., Zahn, R., 1996. Eocene–Oligocene transition in the Southern Ocean: history of water mass circulation and biological productivity. Geology 24 (2), 163–166.

Dupont-Nivet, G., Krijgsman, W., Langereis, C.G., Abels, H.A., Dai, S., Fang, X., 2007. Tibetan plateau aridification linked to global cooling at the Eocene–Oligocene transition. Nature 445, 635–638.

Ennyu, A., Arthur, M.A., Pagani, M., 2002. Fine-fraction carbonate stable isotopes as indicators of seasonal shallow mixed-layer paleohydrography. Marine Micropaleontology 46, 317–342.

Falkowski, P.G., Katz, M.E., Knoll, A.H., Quigg, A., Raven, J.A., Schofield, O., Taylor, F.J.R., 2004. The evolution of modern eukaryotic phytoplankton. Science 305, 354–360.

Farrimond, P., Eglinton, G., Brassell, S.C., 1986. Alkenones in Cretaceous black shales, Blake-Bahama Basin, western North Atlantic. Organic Geochemistry 10, 897–903.

Finkel, Z.V., Katz, M.E., Wright, J.D., Schofield, O.M.E., Falkowski, P.G., 2005. Climatically driven macroevolutionary patterns in the size of marine diatoms over the Cenozoic. PNAS 102 (25), 8927–8932.

Fujiwara, S., Tsuzuki, M., Kawachi, M., Minaka, N., Inouye, I., 2001. Molecular phylogeny of the Haptophyta based on the rbcL gene and sequence variation in the spacer region of the Rubisco operon. Journal of Phycology 37, 121–129.

Haidar, A.T., Thierstein, H., 2001. Coccolithophore dynamics off Bermuda (N. Atlantic). Deep-Sea Research II 48, 1925–1956.

Henderiks, J., 2008. Coccolithophore size rules — reconstructing ancient cell geometry and cellular calcite quota from fossil coccoliths. Marine Micropaleontology. doi:10.1016/j.marmicro.2008.01.005 (Article in Press, available online 26-01-2008).

Henderiks, J., Pagani, M., 2007. Refining ancient carbon dioxide estimates: significance of coccolithophore cell size for alkenone-based pCO_2 records. Paleoceanography 22 (PA3202). doi:10.1029/2006PA001399.

Henderiks, J., Törner, A., 2006. Reproducibility of coccolith morphometry: evaluation of spraying and smear slide preparation techniques. Marine Micropaleontology 58, 207–218.

Hulburt, E.M., 1985. Adaptation and niche breadth of phytoplankton species along a nutrient gradient in the ocean. Journal of Plankton Research 7, 581–594.

Laws, E.A., Popp, B.N., Bidigare, R.R., Kennicutt, M.C., Macko, S.A., 1995. Dependence of phytoplankton carbon isotopic composition on growth rate and $[CO_2]_{aq}$: theoretical considerations and experimental results. Geochimica et Cosmochimica Acta 59, 1131–1138.

Lowenstein, T.K., Demicco, R.V., 2006. Elevated Eocene atmospheric CO_2 and its subsequent decline. Science 313, 1928.

Mackensen, A., Ehrmann, W.U., 1992. Middle Eocene through Early Oligocene climate history and paleoceanography in the Southern Ocean: stable oxygen and carbon isotopes from ODP Sites on Maud Rise and Kerguelen Plateau. Marine Geology 108, 1–27.

Marlowe, I.T., Brassell, S.C., Eglinton, G., Green, J.C., 1990. Long-chain alkenones and alkyl alkenoates and the fossil coccolith record of marine sediments. Chemical Geology 88 (3–4), 349–375.

Medlin, L.K., Sáez, A.G., Young, J.R., 2007. A molecular clock for coccolithophores and implications for selectivity of phytoplankton extinctions across the K/T boundary. Marine Micropaleontology. doi:10.1016/j.marmicro.2007.08.007 (Article in Press, available online 10-09-2007).

Miller, K.G., Berggren, W.A., Zhang, J., Palmer-Julson, A.A., 1991. Biostratigraphy and isotope stratigraphy of Upper Eocene mikrotektites at Site 612: how many impacts? Palaios 6, 17–38.

Nilsen, E.B., Anderson, L.D., Delaney, M.L., 2003. Paleoproductivity, nutrient burial, climate change and the carbon cycle in the western equatorial Atlantic across the Eocene/Oligocene boundary. Paleoceanography 18 (3). doi:10.1029/2002PA000804.

Pagani, M., Arthur, M.A., Freeman, K.H., 1999. Miocene evolution of atmospheric carbon dioxide. Paleoceanography 14 (3), 273–292.

Pagani, M., Zachos, J.C., Freeman, K.H., Tripple, B., Bohaty, S., 2005. Marked decline in atmospheric carbon dioxide concentrations during the Paleogene. Science 309, 600–603.

Persico, D., Villa, G., 2004. Eocene–Oligocene calcareous nannofossils from Maud Rise and Kerguelen Plateau (Antarctica): paleoecological and paleoceanographic implications. Marine Micropaleontology 52, 153–179.

Pielou, E.C., 1969. An Introduction to Mathematical Ecology. Wiley, New York, N.Y. 286 pp.

Popp, B.N., Laws, E.A., Bidigare, R.R., Dore, J.E., Hanson, K.L., Wakeham, S.G., 1998. Effect of phytoplankton cell geometry on carbon isotopic fractionation. Geochimica et Cosmochimica Acta 62, 69–77.

Raven, J.A., 1998. The twelfth Tansley Lecture. Small is beautiful: the picophytoplankton. Functional Ecology 12, 503–513.

Raven, J.A., Johnston, A.M., 1991. Mechanisms of Inorganic-Carbon Acquisition in Marine Phytoplankton and Their Implications for the use of other Resources.

Rost, B., Riebesell, U., Burkhardt, S., Sültemeyer, D., 2003. Carbon acquisition of bloom-forming marine phytoplankton. Limnology and Oceanography 48 (1), 55–67.

Sáez, A.G., Probert, I., Young, J.R., Edvardsen, B., Eikrem, W., Medlin, L.K., 2004. A review of the phylogeny of the Haptophyta. In: Thierstein, H.R., Young, J. (Eds.), Coccolithophores: From Molecular Processes to Global Impact. Springer-Verlag, Berlin Heidelberg, pp. 251–269.

Shackleton, N.J., Crowhurst, S.J., Weedon, G.P., Laskar, J., 1999. Astronomical calibration of Oligocene–Miocene time. Philos. Trans. R. Soc. Lond. 357, 1907–1929.

Spencer-Cervato, C., 1999. The Cenozoic deep sea microfossil record: explorations of the DSDP/ODP sample set using the Neptune Database. Palaeontologia Electronica 2 (2) http://www-odp.tamu.edu/paleo/1999_2/neptune/plain.htm.

Tortell, P.D., 2000. Evolutionary and ecological perspectives on carbon acquisition in phytoplankton. Limnology and Oceanography 45 (3), 744–750.

Volkman, J.K., 2000. Ecological and environmental factors affecting alkenone distributions in seawater and sediments. Geochemistry, Geophysics, Geosystems 1 paper no. 2000GC000061.

Wright, J.D., 2001. Cenozoic climate — oxygen isotope evidence. In: Steele, J., Thorpe, S., Turekian, K. (Eds.), Encyclopedia of Ocean Sciences. Academic Press, London, pp. 415–425.

Young, J.R., 1998. Neogene. In: Bown, P. (Ed.), Calcareous Nannofossil Biostratigraphy. Chapman & Hall, Cambridge, pp. 225–265.

Young, J.R., Didymus, J.M., Bown, P.R., Prins, B., Mann, S., 1992. Crystal assembly and phylogenetic evolution in heterococcoliths. Nature 356, 516–518.

Zachos, J., Pagani, M., Sloan, L., Thomas, E., Billups, K., 2001. Trends, rhythms, and aberrations in global climate 65 Ma to present. Science 292, 686–693.

Zachos, J.C., Quinn, T.M., Salamy, K.A., 1996. High-resolution (10^4 years) deep-sea foraminiferal stable isotope records of the Eocene–Oligocene climate transition. Paleoceanography 11 (3), 251–266.

Zanazzi, A., Kohn, M.J., MacFadden, B.J., Terry, D.O.J., 2007. Large temperature drop across the Eocene–Oligocene transition in central America. Nature 445, 639–642.